The Research Council of Norway (NFR)

NORSAR

NORSAR Scientific Report No. 1-94/95

Semiannual Technical Summary

1 April - 30 September 1994

Kjeller, November 1994

APPROVED FOR PUBLIC RELEASE, DISTRIBUTION UNLIMITED

7.5 Mislocation vectors for small aperture arrays - a first step towards calibrating GSETT-3 stations

Introduction

At NORSAR small aperture arrays have been used for many years to locate seismic events either with onsets at single arrays or with a common interpretation of detections from all available arrays. In this context automatically calculated ray parameter and azimuth values play an important role. It is well known that some observed data show systematic deviations from theoretically expected values, and it is also well known that single data from known source regions show a large scatter. Whatever the reason is for these deviations, they influence the quality of all event locations based on automatically estimated parameters. In this study the phrase "slowness" is always used for the total length of the slowness vector derived from ray parameter and azimuth. Estimation of systematic slowness deviations and statistical information about the scatter of individually measured slowness values are part of the generally needed calibration of all seismic stations of the GSETT-3 network to correct the input to the location procedures. Therefore the data base of all detected phases from all six small aperture arrays for which data are recorded and processed at NORSAR, was investigated to search for systematic patterns in slowness deviations.

Data bases used

At NORSAR the earliest automatically estimated fk-results are available since Jan 1, 1989. To obtain deviations from theoretically expected values a list of reference events is needed. Therefore such a list was compiled for the time period Jan 1, 1989 to June 30, 1994, which was chosen as the end time of this study. Main sources for this list were the bulletins of ISC and PDE. But because these bulletins are not complete for all observable smaller events in Europe, the following local and regional catalogues from Europe were added: for Scandinavia the bulletins of the Seismological Institutes in Helsinki and Bergen, a list of confirmed quarry blasts from the Kola peninsula, for Central Europe a local Bulletin of the Vogtland / Western Bohemian region of earthquake swarms, a list of precisely located events from the Polish mining areas, and a list of confirmed quarry blasts in Bavaria / Germany and in the Czech Republic (for details see Table 7.5.1). All these event lists were merged together, and double entries were carefully eliminated. Table 7.5.1 also gives information about the amount of contributions from each source to the final list of 157 825 reference events.

For all these events, their theoretical onset times as well as predicted slowness values were calculated and compared with automatically estimated values from detections at the arrays investigated. The availability of the fk-results is not the same for all arrays and reflects mostly the successive extension of the European array network (Table 7.5.2).

Association of observed onsets with theoretically estimated onsets

To get reliable mislocation vectors the association criteria must be carefully defined. In this study the following procedure was chosen:

a) For each event in the list of reference events azimuth and distance were calculated with respect to the observing arrays.

b) To get an optimum coverage of the slowness space it is of interest to compare all theoretical arrivals with detected onsets. Using distance, depth, and event origin time, the absolute onset times of all seismic phases as included in the IASP91 tables (Kennett and Engdahl, 1991) were calculated for all arrays considered. To reduce the number of erroneous associations some restrictions related to epicentral distance and event magnitude were introduced, some secondary onsets were only associated if an earlier phase of the same event was also associable, and additionally, all theoretical phases to be considered for comparison with observed ones must be separated in time by at least 3 seconds. The list of used phases with the restrictions that apply is given in Table 7.5.3.

c) These list of onsets for every event was then compared with detections and SigPro-results for each array. For GERESS, the SigPro-results from the processing in Bochum since November 9, 1990 were used instead of the results at NORSAR because of completeness and data quality. To define a theoretically expected phase as observed the residual between detected and theoretically estimated onset time must be less than 10 seconds and the absolute slowness residual must be less than 10 s/deg. In the case of more than one detection in this time interval of +/- 10 seconds around the theoretical onset, the onset with the smallest travel time residual and an acceptable slowness residual was associated. Sometimes, onsets of two or more events have approximately the same arrival time at a seismic station and the list of associations had to be checked for such situations. In such cases all associations were discarded from further use.

d) In a final step, the quality of associations was increased by applying even more restrictive criteria. For P-type onsets no association was used with a larger travel time residual than 4 seconds or a slowness residual of more than 4 s/deg. For the investigated crustal S-type onsets these values were increased to 8 seconds and 8 s/deg respectively, because of larger uncertainty of onset time estimates and larger scatter of observed slowness values for S-type onsets. High frequent noise is often interpreted by the automatic fk-analysis as a teleseismic P-phase. To eliminate these errors high frequency (> 4 Hz) onsets with a ray parameter less than 10 s/deg were not used.

Especially the arrays with a smaller aperture (Apatity, FINESS, and Spitsbergen) had a remarkable number of onsets with large slowness residuals due to lower slowness resolution and less redundancy in the data. In contrast, the array with the largest aperture (GERESS) had the smallest loss of associations due to this point. The influence of high frequency noise was relatively equal for all Scandinavian arrays but neglectable for GERESS due to differences in the detector/SigPro recipes at NORSAR and in Bochum. The restriction to smaller travel time residuals reduced the data for all arrays only slightly.

In summary, these restrictions led to a smaller but more stable set of observed mislocation vectors (compare first and second column in Table 7.5.4). Figure 7.5.1 shows for NORESS all 26 083 used slowness values and gives an impression of the coverage of the slowness space and the scatter of the data. On the top all observed slowness values are seen and at the bottom all corresponding theoretical values are plotted. The circular pattern for large slowness values for the theoretical case (bottom part of figure) is associated with the crustal layering in the IASP91 model.

Mean mislocation vectors

Because of the scatter in single observations it became necessary to calculate mean mislocation vectors. For that the slowness space was divided into 1849 bins and all mislocation vectors were averaged per bin. To divide the slowness space into approximately equally sized areas, the size of the bins varied for different ray parameters between 1 s/deg times 30 deg and 2 s/deg times 5 deg. In this study only mislocation vectors are shown which are based on at least 3 observations in one bin (compare Figs. 7.5.1 and Fig. 7.5.6 which show single observations and mean mislocation vectors for NORESS, respectively). Besides the mean mislocation vectors also corresponding standard deviations were calculated for the observed azimuth and ray parameter values. These standard deviations can be used to weight single observations in further studies. Table 7.5.4 gives for all arrays the mean values of the single mislocation vectors and the mean scatter of the ray parameter and azimuth values before and after applying the slowness corrections. This slowness correction amounts to subtracting the mean mislocation vectors from the observed slowness values within each bin. In comparing columns 3 and 6 of Table 7.5.4 one can see the significant reduction of between 25% and 40% for the mean values of the single mislocation vectors after slowness corrections have been applied.

No explicit relation can be given between observation and theory. So two different types of mislocation vectors can be calculated depending on which slowness value was used as reference for defining the corresponding bin. The first type of vector points from the observations (e.g. as in Fig. 7.5.1 on the top) to the most likely "true" value (the theoretical slowness values shown e.g. in Fig 7.5.1 at the bottom) and the second type points from the theoretical slowness (as in Fig. 7.5.1 at the bottom) to the most likely observed value (i.e. the expected slowness value at the array; see, e.g., Fig 7.5.1 on the top). The latter can predict systematic mislocation errors but not the scatter which is caused by too low slowness resolution or noise. The two types of mislocation vectors are useful for different applications. Figs. 7.5.2 - 7.5.7 show the mislocation vectors for each array. For each figure, the top part shows the observed mislocations (first type) and the bottom part the predicted (second type) mislocations. The symbol size corresponds to the number of single mislocation vectors which were observed per bin and the vectors plotted have to be added to the reference value to get the corrected azimuth and ray parameter.

The figures clearly show that for a sufficient coverage of the slowness space with mislocation vectors a long observing period is needed. This is not only because the seismicity distribution of the Earth is changing by time but also gaps due to station problems must be filled. For the two arrays at Apatity and Spitsbergen which have suffered from problems with data quality and data acquisition, an operation period of about 2.5 years is not long

enough. Unfortunately, these two arrays also have the largest problems with low slowness resolution due to their very small aperture. So the estimation of a sufficient set of mislocation vectors will need several more years of data for these arrays. However, the results for the Apatity array can be used as a first approximation and the results for the Spitsbergen array are shown here for completeness.

Finally, the following question was investigated: How relevant are mislocation vectors that are based on automatically estimated slowness values? At the Institute of Geophysics at Bochum many results of the automatic fk-analysis are reviewed by seismologists, and the values are recomputed following inspection of the data. Such reviewed results are available since April 1991 mostly for P-type onsets with a ray parameter less than 10 s/deg (see Table 7.5.2). For this set of data mislocation vectors can also be estimated and compared with the results for the automatic computations. Fig. 7.5.8 shows these mislocation vectors at the bottom for the reviewed data and on top for the corresponding subset of the automatically estimated data from Fig. 7.5.5. The scatter in the reviewed data is about 8% less (see Table 7.5.4 last two rows). But the main features are very similar in the two plots and the differences between the two mislocation sets are mostly for bins with a small number of observations (smaller symbols). This confirms the use of automatically estimated slowness values in location procedures and shows that the mislocation vectors demonstrated in this paper for small aperture arrays are not the result of some arbitrary processes.

Conclusion

Although a large scatter was observed for single mislocations, mean mislocation vectors could be defined and estimated with their standard deviations for all arrays. These mislocation vectors can now be used regularly to correct automatically estimated slowness and azimuth values. A reduction of the scatter for single observations and a correction for mean mislocation errors is especially needed for single array location routines and for IMS like location algorithms. The predicted mislocation vectors are helpful for estimating better values for the GBF-method. These vectors can also be used to investigate systematic deviations between the used velocity model IASP91 and the velocity structure under the arrays.

J. Schweitzer

References

Kennett, B. L. N. and E. R. Engdahl (1991): Travel times for global earthquake location and phase identification, *Geophys. Journ. Int.*, 105, 429-466.

Mykkeltveit, S (1992): Mining explosions in the Khibiny Massif (Kola peninsula of Russia) recorded at the Apatity three-component station, Report PL-TR-92-2253, Phillips Laboratory, Hanscom AFB, Ma, USA.

Bulletin	Time period	Number of events	Remarks
ISC	Jan 1, 1989 - Jul 31, 1992	120 716	
PDE monthly	Mar 1, 1990 - Dec 31, 1993	26 484	
PDE weekly	Jan 1, 1994 - Jun 30, 1994	4 905	
Helsinki	Jan 1, 1989 - Jun 30, 1994	3 429	
Bergen	Jan 1, 1989 - Mar 31, 1994	1 319	
Polish mines	Jun 27, 1990 - Jun 12, 1992	418	P. Wiejacz and J. Niewiadomski (both Polish Academy of Sciences, Warsaw) several pers. communications in 1991 and 1992
Bavarian & Czech quarries	Jan 9, 1991 - Oct 14, 1992	285	Compiled at the Institute of Geophysics at Ruhr-University Bochum, supported by several pers. communications with J. Zednik (Czech Academy of Sciences, Praha) in 1992
Kola quarries	Jun 15, 1991 - Oct 23, 1992	195	Mykkeltveit (1992)
Vogtland	Jan 31, 1991 - Nov 16, 1992	74	Bulletin of the Vogtland / Western Bohemian earthquakes, ed. by H. Neunhoefer, University of Jena
Sum	Jan 1, 1989 - Jun 30, 1994	**157 825**	

Table 7.5.1: Contributions of the different bulletins to the list of reference events.

Array	Analyzed time period
Apatity	May 31, 1992 - Jun 30, 1994
ARCESS	Jan 1, 1989 - Jun 30, 1994
FINESS	Nov 23, 1989 - Jun 30, 1994
GERESS	Oct 17, 1990 - Jun 30, 1994
GERESSr	Apr 22, 1991 - Jun 30, 1994
NORESS	Jan 28, 1989 - Jun 30, 1994
Spitsbergen	Nov 23, 1992 - Jun 30, 1994

Table 7.5.2: Time periods of investigated fk-results for the various small aperture arrays. Additionally, for GERESS a data set of analyst-reviewed fk results could be investigated (GERESSr).

Phase	Restrictions
Pg, Sg	del < 10 deg
PgPg, SgSg	4 deg ≤ del < 10 deg; *
Pb, Sb	del < 15 deg
PbPb, SbSb	4 deg ≤ del < 15 deg; *
Pn, Sn	---
PnPn, SnSn	4 deg ≤ del < 18 deg; (SnSn *)
P, pP, sP	---
PcP, ScP	10 deg ≤ del; mag; *
Pdiff	110 deg ≤ del
pPdiff, sPdiff	110 deg ≤ del; if magnitude < 4.0 then *
PKiKP	del ≥ 80 deg
pPKiKP, sPKiKP	del ≥ 80 deg; if magnitude < 4.0 then *
PKP, pPKP, sPKP, SKP	---
PKKP	del ≥ 30 deg; mag; * P'P' mag; *

Table 7.5.3: Phases for which ray parameter and azimuth values were used in this study to estimate the mislocation vectors. For core phases all branches were used (i.e., ab, bc, and df). mag = phase was used only if event magnitude was not lower than 4.0; * = phase was used only if another earlier onset from the same event was observed. del = distance.

Array	No. of detections		Mean scatter			Mean scatter after slowness corrections		
	Asso-ciated	Used	Slow-ness	Ray para-meters	Azim.	Slow-ness	Ray para-meter	Azim.
			[s/deg]	[s/deg]	[deg]	[s/deg]	[s/deg]	[deg]
Apatity	3 654	1 882	2.77	2.24	19.44	1.66	1.51	14.45
ARCESS	42 521	29 738	1.87	1.65	21.83	1.32	1.11	18.99
FINESS	22 798	15 482	2.20	1.79	23.99	1.59	1.28	21.74
GERESS	23 499	17 852	2.00	1.77	23.97	1.47	1.29	20.64
NORESS	34 987	26 083	2.09	1.85	17.01	1.56	1.36	15.58
Spitsbergen	1 267	253	1.89	1.96	27.46	1.25	0.94	22.73
GERESSr		8 000	1.54	1.28	26.97	1.29	1.08	22.91
GERESSa		10 579	1.66	1.40	30.75	1.42	1.16	26.33

Table 7.5.4: Some numerical results of the mislocation study. GERESSr gives the results for analyst-reviewed P-type onsets (ray parameter <= 10 s/deg) and GERESSa is the corresponding subset of the automatically estimated data from GERESS (see text and Fig. 7.5.8).

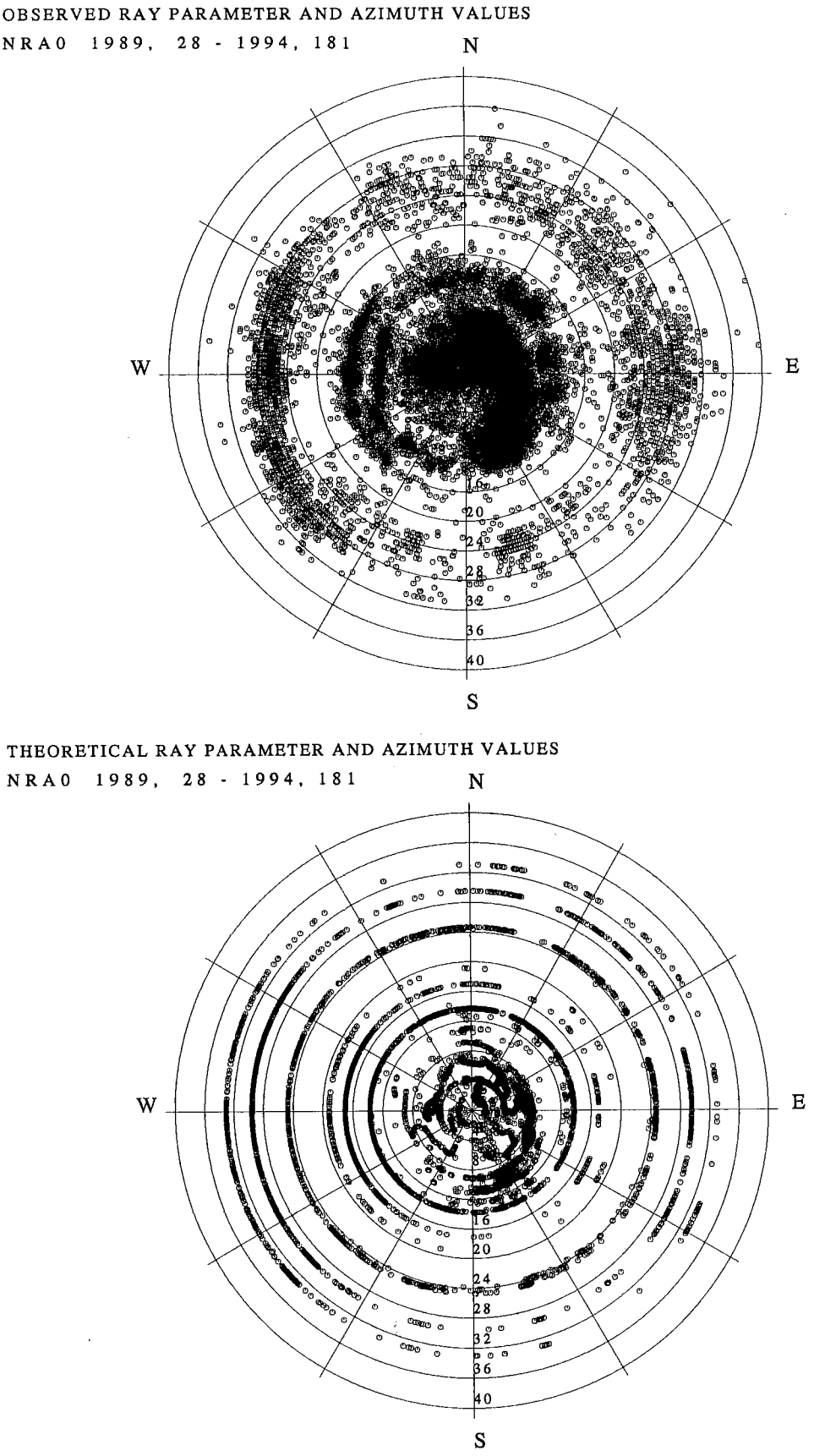

Fig. 7.5.1: The upper plot shows all 26 083 NORESS slowness observations used in this study and at the bottom all corresponding theoretical slowness values are seen.

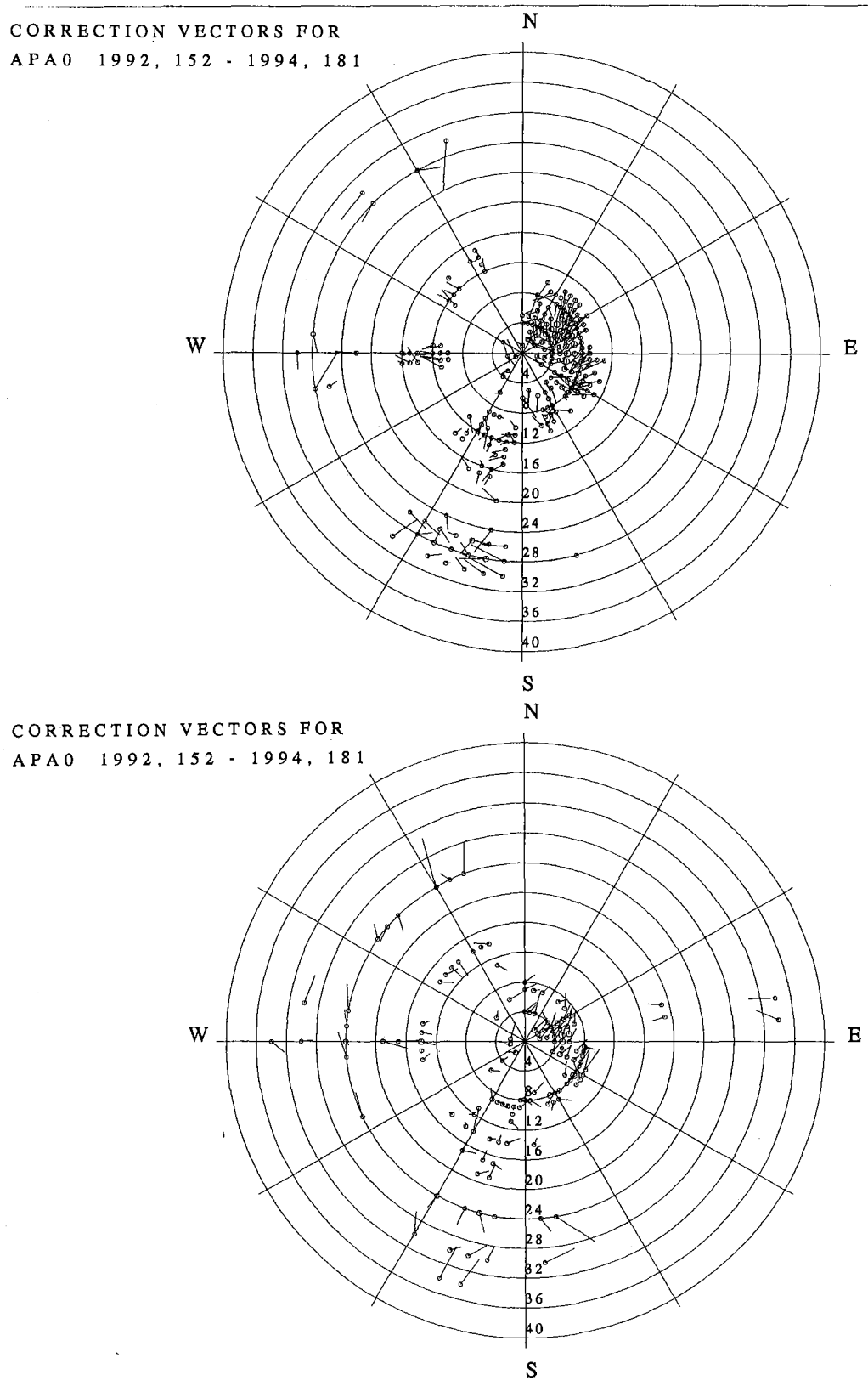

Fig. 7.5.2: The upper plot shows 222 Apatity slowness mislocation vectors relative to the observed values. At the bottom the 134 corresponding mislocation vectors relative to the theoretical values (predicted mislocations) are seen. The symbol size corresponds to the number of single observations per bin. The maximum number of observations per mislocation vector is 25 (top) and 84 (bottom).

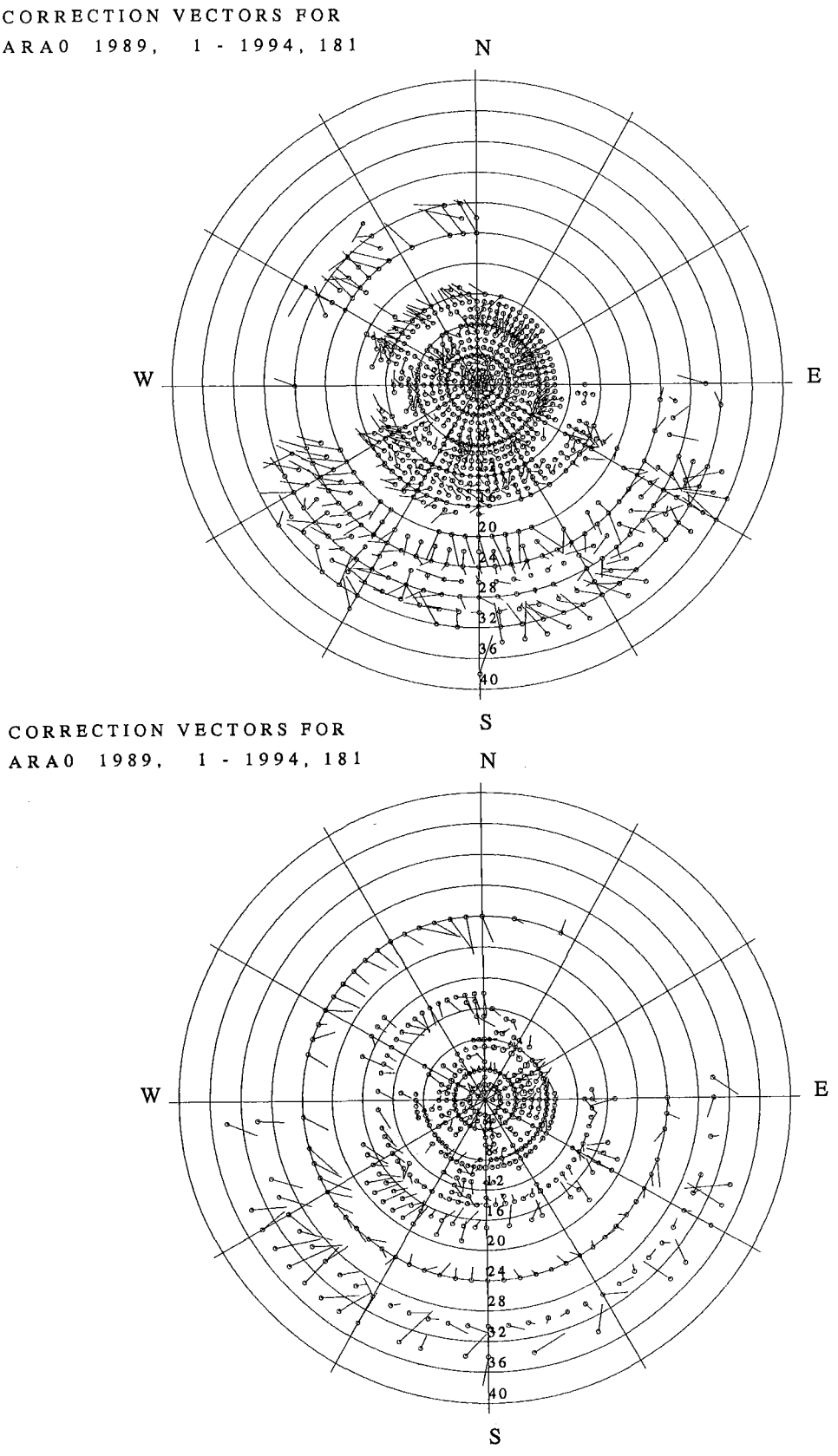

Fig. 7.5.3: As Fig. 7.5.2 but for ARCESS. The number of mislocation vectors is 796 (relative to observation) and 435 (relative to the theory). The maximum number of observations per mislocation vector is 631 (top) and 2419 (bottom).

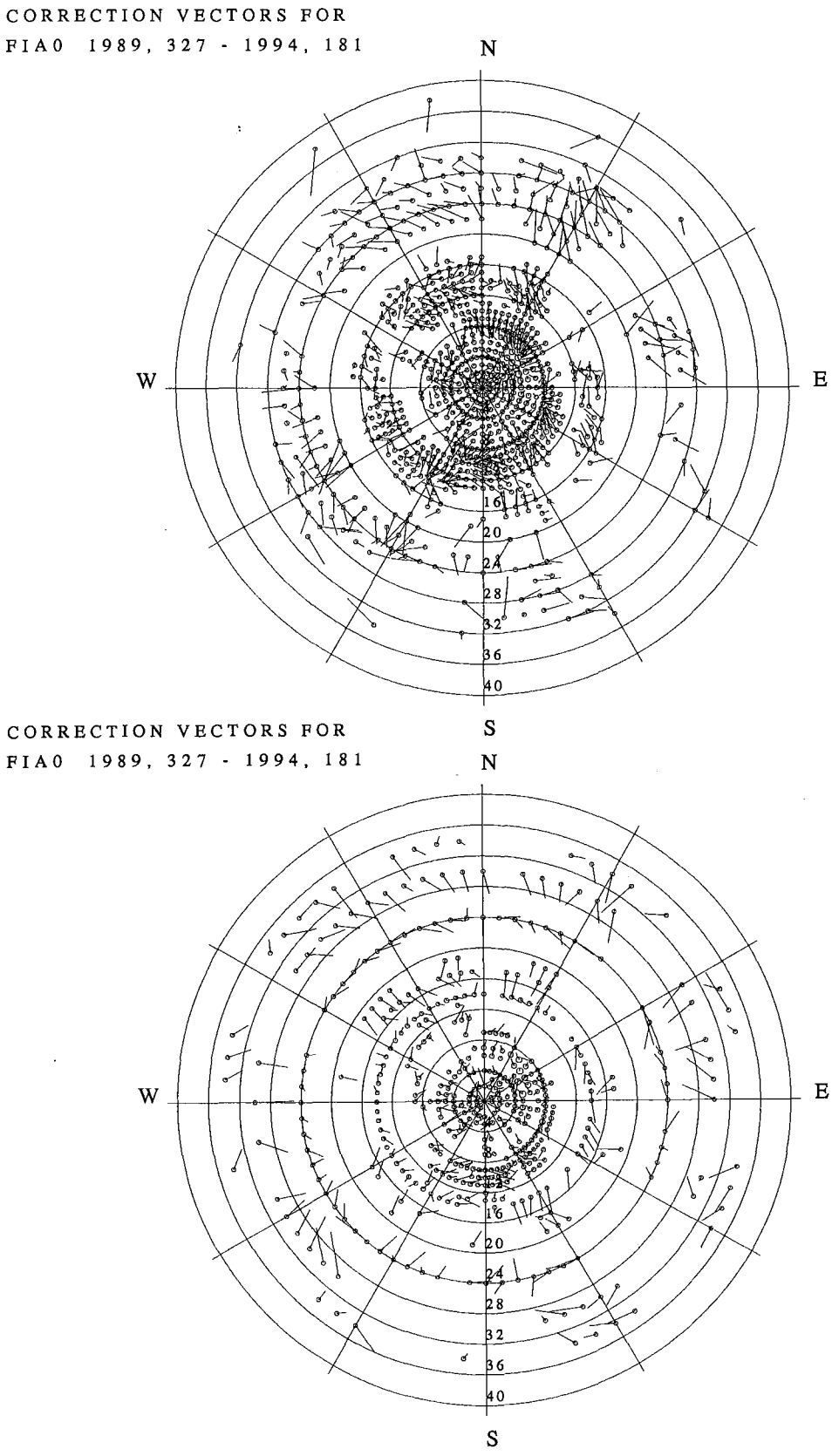

Fig. 7.5.4: As Fig. 7.5.2 but for FINESS. The number of mislocation vectors is 806 (relative to observation) and 446 (relative to the theory). The maximum number of observations per mislocation vector is 298 (top) and 996 (bottom).

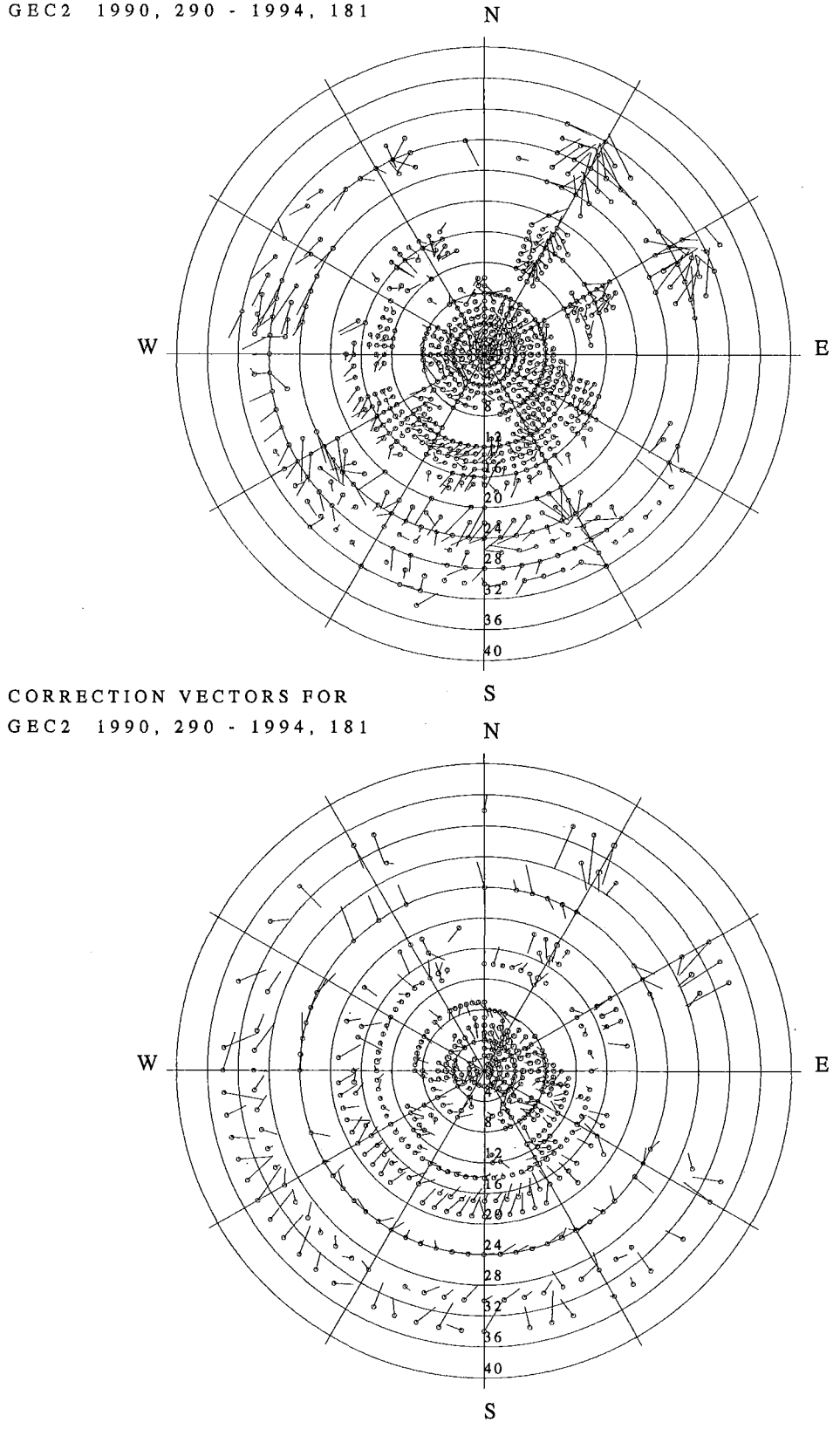

Fig. 7.5.5: As Fig. 7.5.2 but for GERESS. The number of mislocation vectors is 760 (relative to observation) and 469 (relative to the theory). The maximum number of observations per mislocation vector is 325 (top) and 619 (bottom).

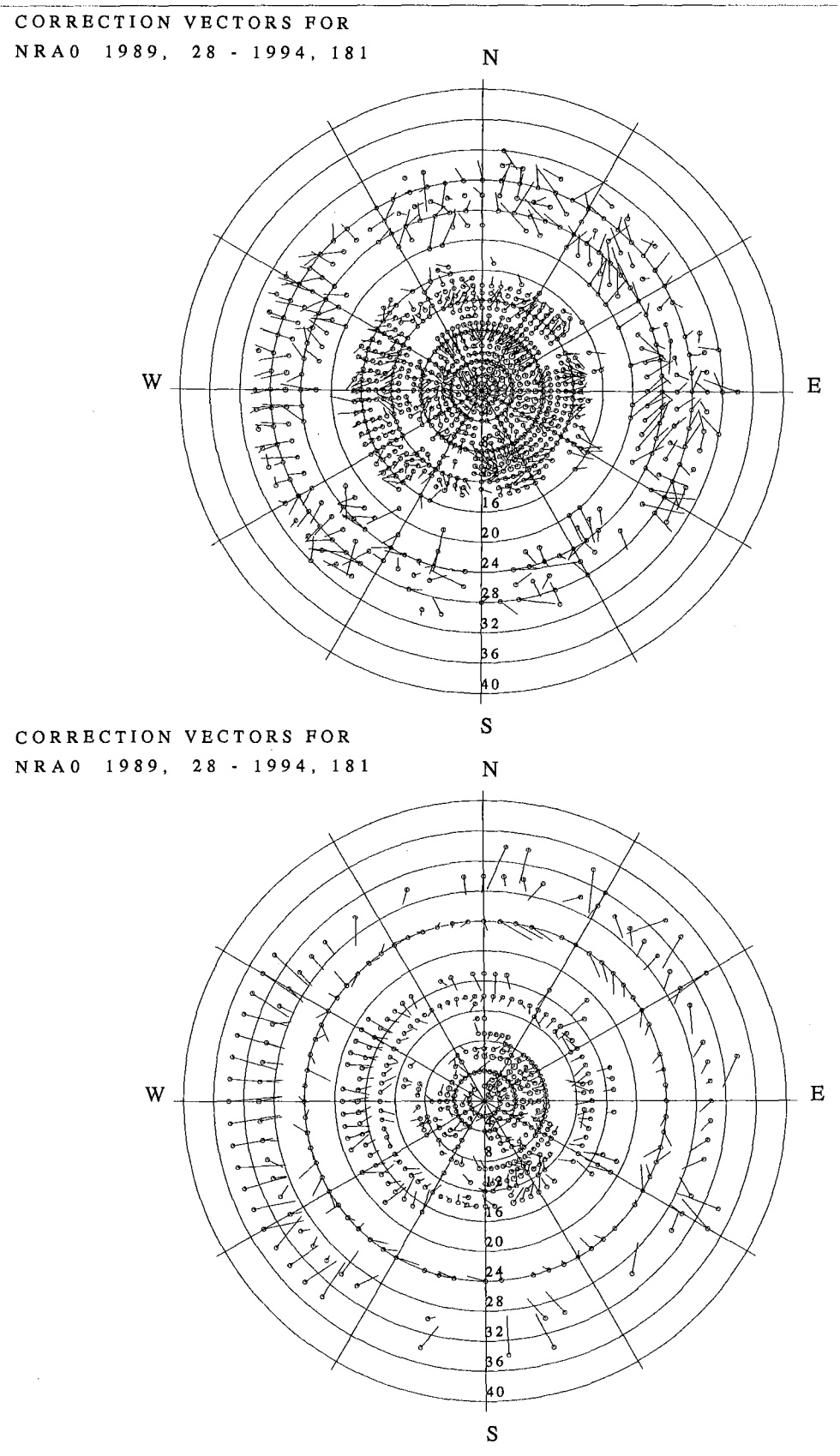

Fig. 7.5.6: As Fig. 7.5.2 but for NORESS. The number of mislocation vectors is 934 (relative to observation) and 497 (relative to the theory). The maximum number of observations per mislocation vector is 614 (top) and 1282 (bottom).

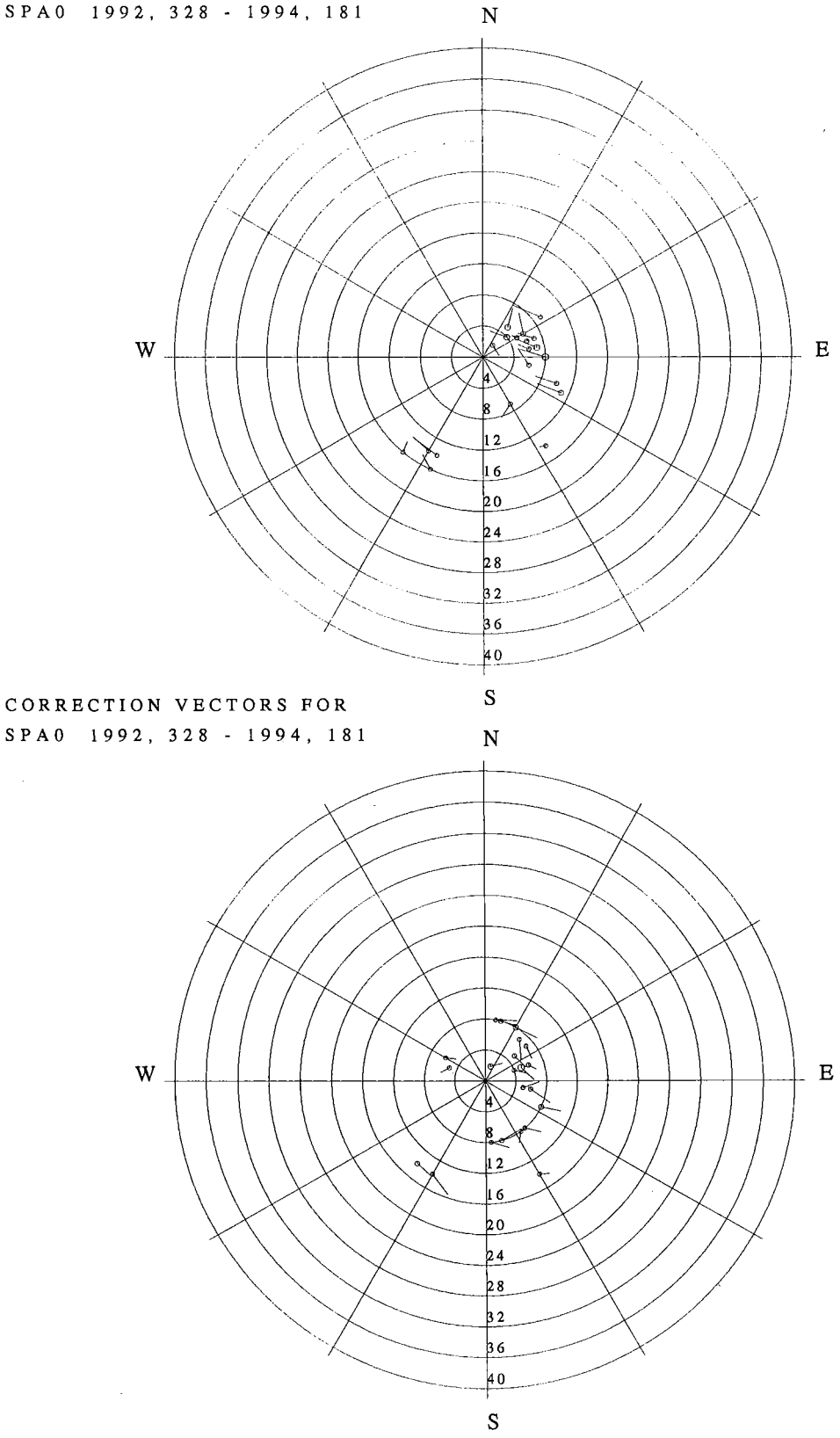

Fig. 7.5.7: As Fig. 7.5.2 but for Spitsbergen. The number of mislocation vectors is 20 (relative to observation) and 22 (relative to the theory). The maximum number of observations per mislocation vector is 6 (top) and 26 (bottom).

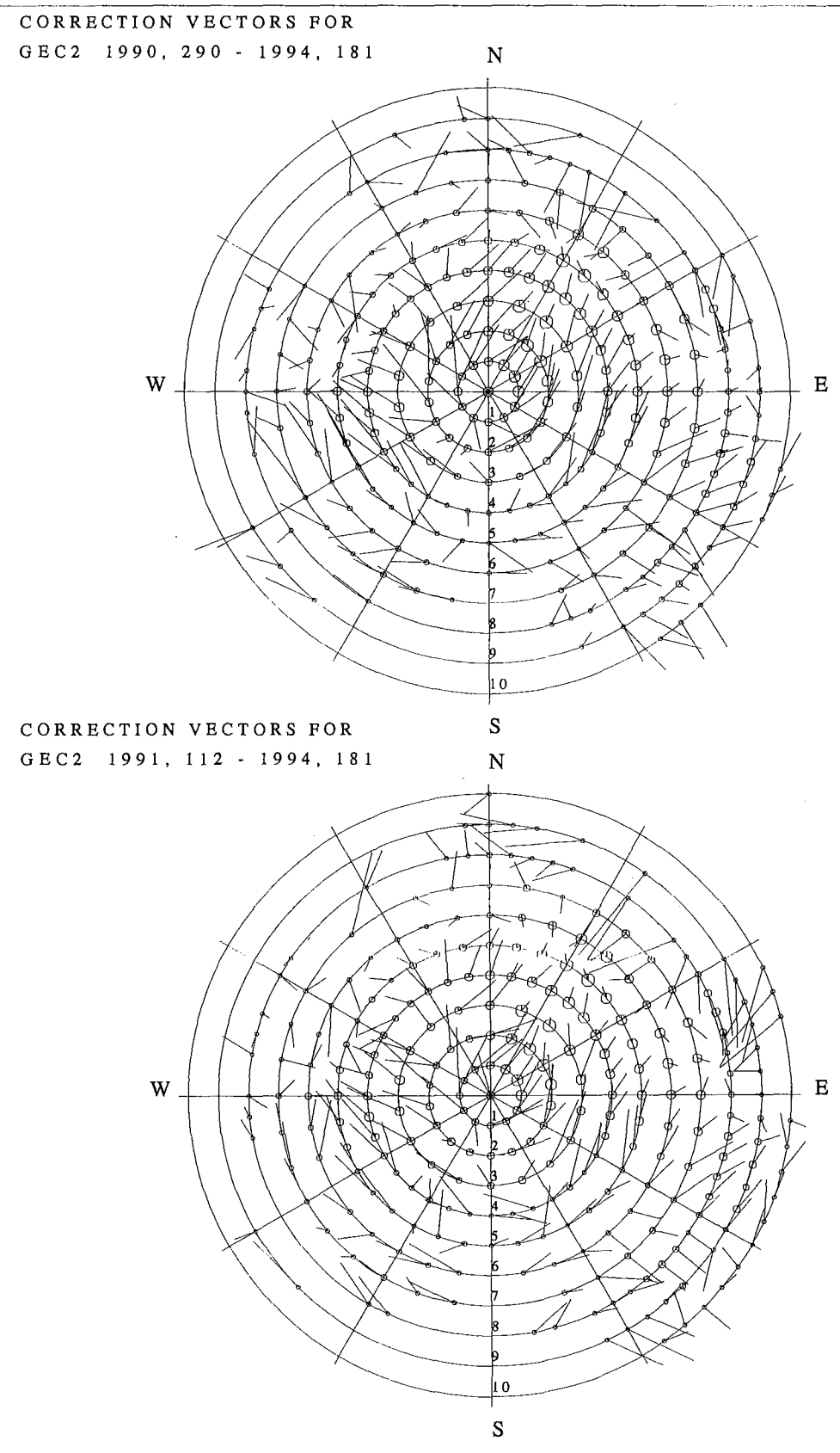

Fig. 7.5.8: Mislocation vectors for GERESS P-type onsets. On the top a subset is shown of the data from Fig. 7.5.5 (top), and at the bottom the mislocation vectors for a collection of GERESS analyst-reviewed slowness values are shown.